Study by Infrared Spectroscopy of Ultrathin Films of Behenic Acid Methyl Ester on Solid Substrates and at the Air/Water Interface

Isabelle Pelletier,[†] Hélène Bourque,[†] Thierry Buffeteau,[‡] Daniel Blaudez,[§] Bernard Desbat,[‡] and Michel Pézolet*,[†]

Centre de Recherche en Science et Ingénierie des Macromolécules, Département de Chimie, Université Laval, Québec, G1K 7P4, Canada, and Laboratoire de Physico-Chimie Moléculaire, UMR 5803 du CNRS, Université Bordeaux I, 33405 Talence, France, and Centre de Physique Moléculaire Optique et Hertzienne, UMR 5798 du CNRS, Université Bordeaux I, 33405 Talence, France

Received: June 13, 2001; In Final Form: November 17, 2001

Ultrathin films of behenic acid methyl ester (BAME) deposited by spin coating on solid substrates or spread at the air/water interface were studied by infrared spectroscopy and Brewster angle microscopy. Anisotropic optical constants of BAME were determined from a transmittance spectrum at normal incidence and a parallel-polarized reflectance spectrum at grazing incidence. A transmittance spectrum recorded at oblique incidence (60°) was used to validate these optical constants. The anisotropic extinction coefficients and the polarized ATR spectra were used to calculate the tilt angle of several transition moments and also the molecular tilt angle of BAME molecules assuming an all-trans conformation of the alkyl chain. The results indicate that the alkyl chain of the fatty acid ester is tilted and that the molecular tilt angle is close to 30°. PM-IRRAS spectra of BAME at the air/water interface were also recorded as a function of the surface pressure. The splitting of the methylene bending mode shows that the all-tans alkyl chains are packed in a quasi-crystalline structure at the air/water interface, even at low surface pressure. This finding was further confirmed by Brewster angle microscopy. Furthermore, the band progression due to the methylene wagging modes was observed for the first time in infrared spectra of a Langmuir monolayer. The simulation of the PM-IRRAS spectrum of a BAME monolayer recorded at 30 mN/m using the optical constants obtained from films prepared by spin coating indicate that, as opposed to the orientation on solid substrates, the alkyl chain of BAME is nearly perpendicular to the air/water interface in Langmuir films.

Introduction

Ultrathin films such as mono- and multilayers are of great interest in many fields such as optics[1], sensors,[2,3] lubricants,[4] coatings, surfactants, etc. These films can be studied at the air/water interface or on solid substrates by different techniques such as fluorescence,[5] Brewster angle[6−9] and atomic force[10−12] microcopies, X-ray and neutron methods,[8,11,13−19] and Fourier transform infrared spectroscopy (FTIR). The latter technique presents several important advantages. First, the shape, intensity and position of the bands of an infrared spectrum are sensitive to the conformation and the structure of various functional groups. Second, FTIR spectroscopy is sensitive enough to study ultrathin films both at the air/water interface and on solid substrates. Finally, infrared spectroscopy gives quantitative information about molecular orientation since the absorption of the infrared radiation depends on the angle between the plane of polarization of the incident light and the transition moment of a given vibration.

Infrared reflection−absorption spectroscopy (IRRAS)[20−28] and polarization modulation infrared reflection−absorption spectroscopy (PM-IRRAS)[29−36] have been used to record infrared spectra of thin films directly at the air/water interface. These techniques are particularly well suited for this purpose since they provide information on the orientation and conformation at the molecular level. Because the detected signal is differential in nature, PM-IRRAS spectra are almost unaffected by the isotropic absorptions of the sample environment, such as water vapor.[30] Moreover, the orientation of the bands with respect to the baseline is directly related to the orientation of the transition moments with respect to the plane of the water subphase.[29,32] Attenuated total reflectance (ATR), transmission and IRRAS techniques can be used to obtain spectra of films deposited on solid substrates. ATR spectroscopy is one of the best tools for that purpose because it gives spectra with excellent signal-to-noise ratio.[37−44] IRRAS spectroscopy on a metallic surface is also a very interesting technique for orientation studies because it is exclusively sensitive to components of the transition moments that are perpendicular to the plane of the film.

Molecular orientation of ultrathin films has gained a lot of attention recently due to its impact on the macroscopic properties of the film. Different techniques have been used to determine molecular orientation in thin films. For example, Brewster angle microscopy (BAM),[6] X-ray, and neutron reflection[8] provide information on the film thickness and thus on the molecular tilt angle. Orientation has also been determined efficiently by infrared spectroscopy from either polarized transmission,[37,38,45] IRRAS,[45−48] PM-IRRAS[33] or polarized ATR[37−42,44] experiments. However, when the orientation distribution is not uniaxial or when the symmetry of the molecules is not cylindrical, infrared spectra are difficult to interpret quantitatively in term

* To whom correspondence should be addressed. E-mail: michel.pezolet@chm.ulaval.ca. Fax: (418) 656-7916.
[†] Université Laval.
[‡] Laboratoire de Physico-Chimie Moléculaire, Université Bordeaux I.
[§] Centre de Physique Moléculaire Optique et Hertzienne, Université Bordeaux I.

10.1021/jp012236a CCC: $22.00
Published on Web 02/02/2002

of the molecular orientation. A new method has recently been developed by Buffeteau et al. to overcome these difficulties.[36,44,49] In this method, the anisotropic optical constants (in-plane and out-of-plane complex refractive indexes) of the film are determined from a normalized transmittance spectrum at normal incidence and a parallel-polarized reflectance spectrum at grazing incidence. From these optical constants, it is possible to calculate the average orientation of each transition moment and of the molecules when their conformation is known. Moreover, infrared spectra of thin films deposited onto different substrates can be simulated under several experimental conditions (angle of incidence, polarization, ...). This method has already been used to study the molecular orientation of cadmium arachidate (CdAr)[49] and poly(γ-benzyl-L-glutamate) (PBG)[44] molecules deposited on solid substrates or at the air/water interface.

In this paper, we have studied the molecular orientation of behenic acid methyl ester (BAME) deposited onto several substrates. BAME has been chosen because it forms very well organized films on solid substrates and at the air/water interface. Indeed, it has been shown by Flach et al. that in the IRRAS spectrum of a BAME monolayer at the air/water interface, the bands due to the methylene scissoring and rocking modes are splitted indicating a quasi-crystalline structure of the film with the hydrocarbon chains in an all-trans conformation.[28] In this study, the anisotropic optical constants have been determined from ultrathin films of BAME deposited by spin-coating onto solid substrates in order to calculate the oscillator strength of the methylene stretching modes and the orientation of the alkyl chains. The anisotropic optical constants obtained were also used to simulate polarized ATR spectra of BAME deposited on a germanium substrate and the PM-IRRAS spectrum of BAME at the air/water interface, thus allowing the comparison of the orientation of the alkyl chain of the methyl ester in different environments. The organization of a BAME monolayer at the air/water interface has also been investigated by Brewster angle microscopy.

Materials and Method

Sample Preparation. BAME and HPLC grade chloroform were purchased from Sigma-Aldrich and used without any further purification. BAME with a deuterated polar head has been synthesized by esterification of behenic acid with deuterated methanol. Deuterated BAME was purified by recrystallization. Ultrathin films of BAME were formed by spreading 100 μL of a 4 mg/mL solution in chloroform onto the substrate and then spinning it at a rate of 3500 rpm for 30 s. Films were spin-coated on gold mirrors, BaF_2 windows and germanium ATR crystals. The ATR crystals were parallelograms (45°) of 50 $\times$ 20 $\times$ 2 mm, allowing 24 internal reflections. Before deposition, the germanium substrates were cleaned with chloroform and put in a plasma cleaner (Harrick Scientific, Ossining, NY) for 2 min. Gold mirrors and BaF_2 substrates were cleaned with a 1% solution of Hellmanex (Hellma, Concord, CA) and then rinsed with ultrapure water.

BAME monolayer at the air/water interface was obtained by spreading 30 μL of a 1 mg/mL solution in chloroform onto a ultrapure water subphase in a Nima 611 trough (Nima Technology, Coventry, U.K.). After an equilibration period allowing solvent evaporation, the monolayer was compressed at a rate of 5 cm^2/min. Brewster angle microscopy and PM-IRRAS measurements were performed at several surface pressures (π) as well as at 0 mN/m (after spreading of the BAME solution).

Brewster Angle Microscopy Measurements. The morphology of BAME monolayers was observed using a Brewster angle microscope (NFT BAM2*plus*, Göttingen, Germany). The microscope was mounted on a Nima trough and was equipped with a frequency-doubled Nd:Yag laser (532 nm, 20 mW), a polarizer, an analyzer and a CCD camera. The spatial resolution of the BAM was about 2 μm, and the size of an image was 625 $\times$ 500 μm.

FTIR Measurements. Infrared spectra were recorded using either Magna 760, Nexus 670 or 870 Fourier Transform infrared spectrometers (Nicolet Instruments, Madison, WI) with either MCT or DTGS detectors. To obtain ATR spectra, the germanium crystals were placed in a vertical ATR accessory (Harrick Scientific, Ossining, NY). A motorized rotating ZnSe wire-grid polarizer (Specac, Orpington, U.K.) was positioned in front of the sample to obtain polarized spectra without breaking the purge of the spectrometer. For the ATR spectra, 250 scans were sufficient to achieve a high signal-to-noise ratio. Polarized transmittance experiments at normal and oblique incidence (60°) were obtained by co-adding 200 scans. P-polarized IRRAS spectra at an incidence angle of 80° were recorded by co-adding 400 scans. Experimental setup for PM-IRRAS measurements at the air/water interface has been described elsewhere.[29,30] PM-IRRAS spectra of covered S(d) and uncovered S(0) water surface were recorded at an angle of incidence of 75° by co-adding 300 scans at a resolution of 4 cm^{-1}. Normalized PM-IRRAS spectra S(d)/S(0) are presented in this paper. These spectra were obtained at an angle of incidence of 75° with s-polarized light by setting the photoelastic modulator for maximum efficiency either at 2000 or 1450 cm^{-1}.

Thickness Measurements. The thickness of the spin-coated BAME films deposited on different substrates was measured with a single wavelength (λ = 632.8 nm) Gaertner (L116B) ellipsometer using a refractive index of 1.41.[28] The thickness of the films was found to vary from one substrate to another. The thickness was 175 $\pm$ 5 Å on gold, 190 $\pm$ 10 Å on BaF_2 and 230 $\pm$ 5 Å on germanium.

Optical Constants Determination. To evaluate the anisotropic optical constants of ultrathin films in the space coordinate system (*x*, *y* and *z*), we have used a calculation procedure that allows a direct determination of the refractive indexes and extinction coefficients from experimental FTIR spectra. The optical constants along the *x*, *y* and *z* directions of the substrate are calculated using an iterative procedure based on the inversion of spectral simulations. Details of this procedure are given elsewhere.[36,44,49] The optical constants in the plane of the layer (n_x, k_x and n_y, k_y) are determined from polarized transmittance spectra at normal incidence of the thin film deposited on an infrared transparent substrate (BaF_2 window). Indeed, in this case, the electric vector is in the surface plane and only the (*x*, *y*) components of the transition moment can be observed. On the other hand, the optical constants out of the plane of the layer (n_z, k_z) are determined from a p-polarized IRRAS spectrum of the thin film deposited on a metallic substrate, usually a gold mirror. In this case, the electric vector is quasi perpendicular to the surface and interacts almost exclusively with the normal component (*z*) of the transition moments of molecules. This calculation method has several advantages. In addition to providing the wavenumber dependence of the complex refractive indexes (*n* and *k*), it allows the calculation of the average orientation of each transition moment and of the molecules when their conformation is known. Furthermore, the anisotropic optical constants allow the simulation of spectra under various experimental conditions (uniaxial or biaxial orientation, incidence angle, light polarization, substrate, thickness of the film, environment, etc.). By comparing the experimental and simu-

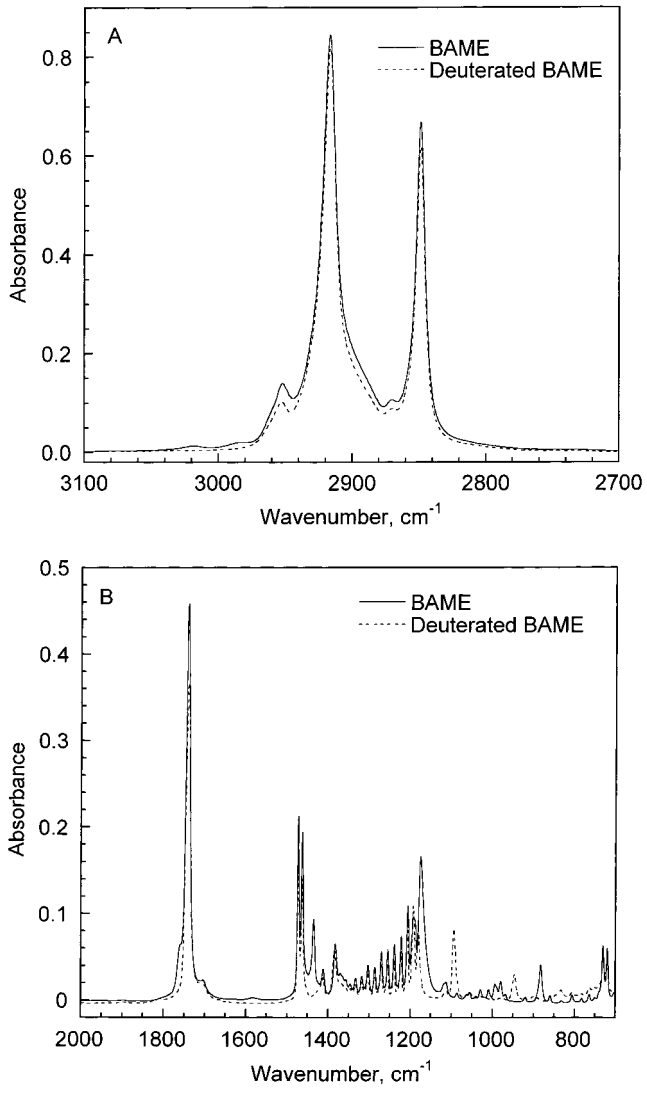

Figure 1. ATR spectra of thick isotropic films of deuterated and nondeuterated BAME in (A) the 3100−2700 cm^{-1} region and (B) the 2000−700 cm^{-1} region.

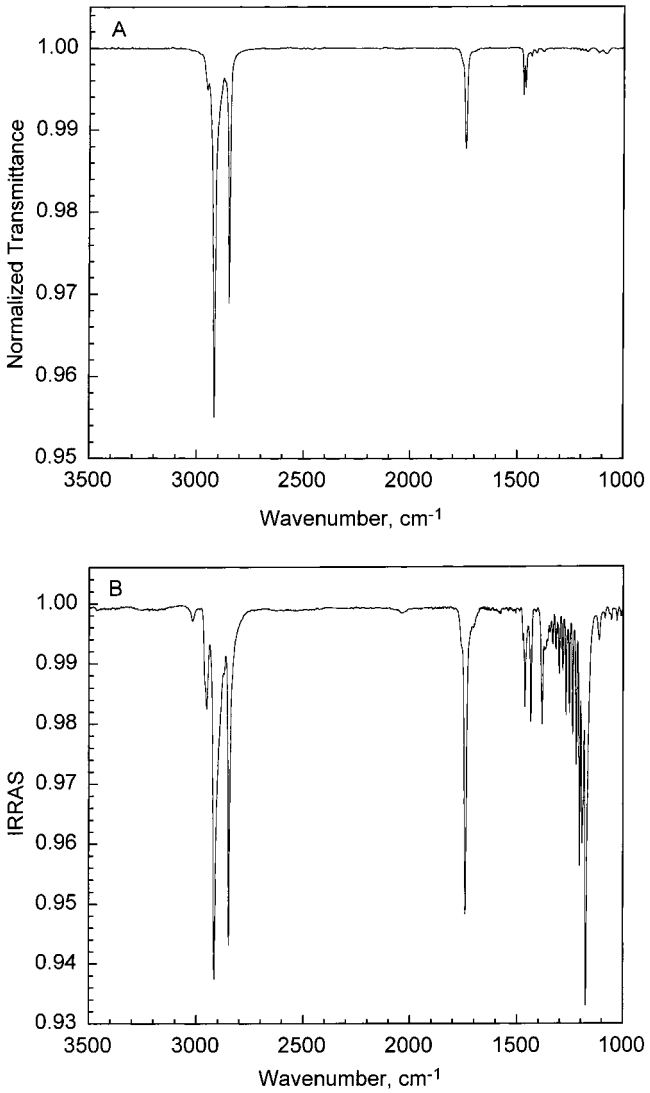

Figure 2. (A) Transmittance spectrum of BAME on BaF_2 at normal incidence and (B) IRRAS spectrum of BAME on gold mirror.

lated spectra, the spectral changes due to optical and chemical effects can be distinguished. The major limitation of this method is that the molecular orientation of the film must be the same on gold and on BaF_2 substrates.

Results

Band Assignment in the Infrared Spectrum of BAME. Figure 1 shows the ATR spectrum of thick isotropic film of BAME in the 2700 to 3100 cm^{-1} and 700 to 2000 cm^{-1} spectral ranges. The high-frequency region is characterized by two strong bands due to the antisymmetric ($\nu_a(CH_2)$) and symmetric ($\nu_s(CH_2)$) methylene C−H stretching modes at 2918 and 2850 cm^{-1}. This spectrum also shows two weak bands at 2952 and 2871 cm^{-1}, assigned to the antisymmetric ($\nu_a(CH_3)$) and symmetric ($\nu_s(CH_3)$) stretching modes of the methyl of the alkyl chain. The low-frequency region contains bands due to the C═O stretching vibration of the ester group at 1739 cm^{-1} and doublets due to the methylene bending ($\delta(CH_2)$) mode at 1473−1463 cm^{-1} and methylene rocking ($r(CH_2)$) mode at 730−719 cm^{-1}. These splittings are caused by a crystal field effect and indicate that the film adopts a quasi-crystalline structure with either an orthorhombic or a monoclinic subcell packing of the alkyl chains.[50] The spectrum also clearly shows several bands in the 1200−1360 cm^{-1} region due to the wagging and twisting modes of the methylene groups. The presence of this band progression and the frequencies of the $\nu_a(CH_2)$ and $\nu_s(CH_2)$ modes indicate that the alkyl chain of BAME is in the all-trans conformation. To distinguish the bands arising from the methyl group of the polar head and that of the alkyl chain, molecules with a deuterated polar head were synthesized. The spectrum of the deuterated BAME is also shown (in dashed line) in Figure 1. The two weak bands located at 3019 and 2985 cm^{-1} bands observed in the nondeuterated spectrum shift to 2269 and 2245 cm^{-1}, respectively, in the spectrum of the deuterated sample (not shown), indicating that they arise from the methyl group of the polar head. Other bands at 1435 and 1174 cm^{-1} shift to 1093 and 946 cm^{-1}, respectively, in the spectrum of deuterated BAME. The first one is assigned to the symmetric bending vibration of the methyl group of the polar head while the second one, is assigned to the C−O−C stretching vibration.

Calculation and Validation of the Optical Constants. To verify the in-plane symmetry of the BAME film deposited by spin coating onto the BaF_2 substrate, polarized transmittance spectra at normal incidence were first recorded. The vertical and horizontal polarized spectra were identical, indicating that the symmetry of the film was uniaxial. Thus, the in-plane optical constants of BAME were determined from the unpolarized transmittance spectrum shown in Figure 2A. On the other hand,

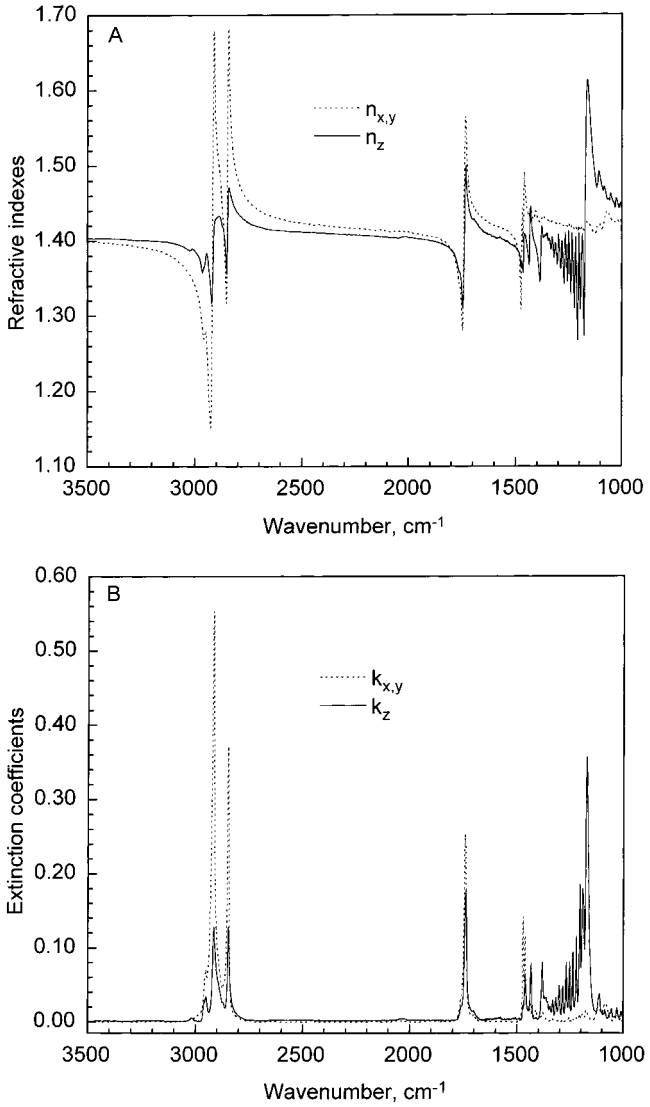

Figure 3. (A) Refractive indexes and (B) extinction coefficients of BAME calculated from the spectra of Figure 2.

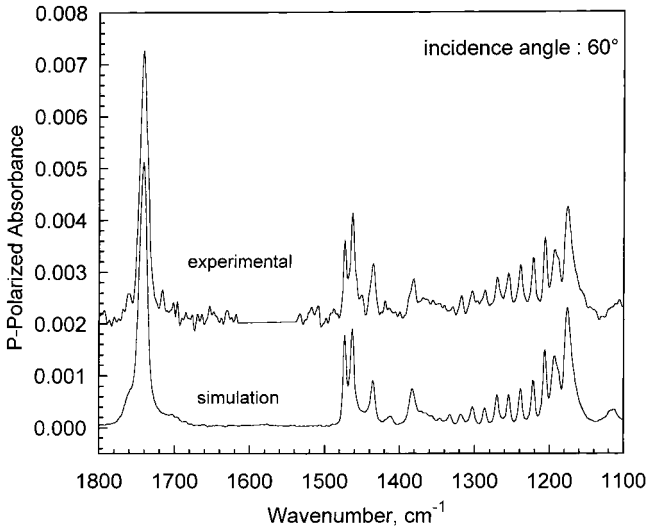

Figure 4. Experimental and simulated p-polarized transmittance spectra of BAME at an incidence angle of 60°.

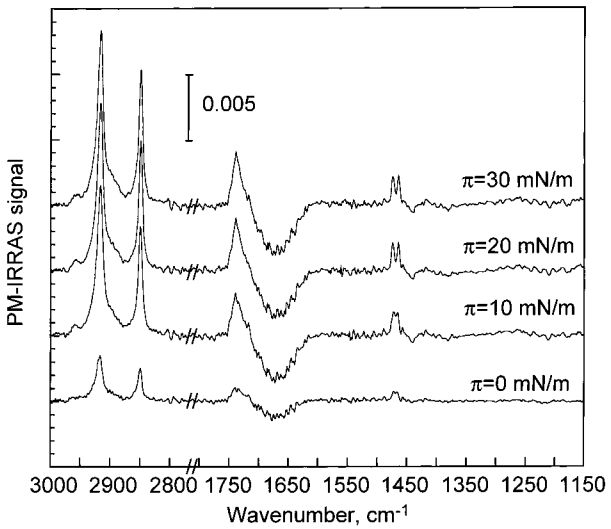

Figure 5. PM-IRRAS spectra of a monolayer of BAME at the air/water interface at different surface pressures. To record these spectra, the photoelastic modulator was set to introduced a maximum dephasing at 1450 cm^{-1}.

the out-of-plane constants were calculated using a p-polarized IRRAS spectrum of the film deposited on a gold mirror. This spectrum is shown in Figure 2B. The anisotropic refractive indices and extinction coefficients calculated from the transmittance and IRRAS spectra are shown in Figure 3A,B, respectively. These calculations were done using a value of n_∞ (index of refraction in the visible) of 1.41.[28] A more detailed analysis of these data will be presented in the discussion section. To validate these optical constants, a p-polarized transmittance spectrum was recorded at oblique incidence (60°) and compared to the simulated one. As seen in Figure 4, the simulated spectrum reproduces very well that obtained experimentally, in the 1000−2000 cm^{-1} region. This shows unambiguously that the relative value of the optical constants in the plane and out of the plane of the film of BAME is correct and that the molecular orientation of the BAME is the same on gold and on BaF_2 substrates.

PM-IRRAS and Brewster Angle Microscopy of BAME at the Air/Water Interface. PM-IRRAS allows the recording of the spectrum of a monolayer directly at the air/water interface. This technique gives spectra in which the orientation of the observed bands with respect to the baseline depends on the tilt angle of their transition moment. For an angle of incidence greater than the Brewster angle (i.e., 53° at the air/water interface), a transition moment oriented perpendicular to the plane of the film gives rise to a negative band while a transition moment lying in the plane of the film gives rise to a positive band. Figure 5 shows the PM-IRRAS spectra of BAME in the 2800−3000 and 1150−1800 cm^{-1} regions for various surface pressures. The bands due to the alkyl chain and the polar headgroup are observed immediately after spreading of the BAME solution on the Langmuir trough ($\pi \approx 0$ mN/m). The intensity of these bands increases when the surface pressure increases. As seen in this figure, the bands due to the methylene stretching ($\nu_a(CH_2)$ and $\nu_s(CH_2)$) and bending ($\delta(CH_2)$) modes are positive indicating that the transition moment associated with these bands mostly lie in the plane of the film. The splitting of the $\delta(CH_2)$ band is clearly visible on PM-IRRAS spectra, even at low surface pressure, showing that the film adopts a quasi-crystalline structure at the air/water interface. The presence of this doublet at very low surface pressure shows that molecules spontaneously form ordered domains at the air/water interface. The 1739 cm^{-1} band due to the C═O stretching mode and the 1411 cm^{-1} band due to the antisymmetric bending of the terminal methyl of the alkyl chain are also positive, indicating that their transition moments are also parallel to the plane of

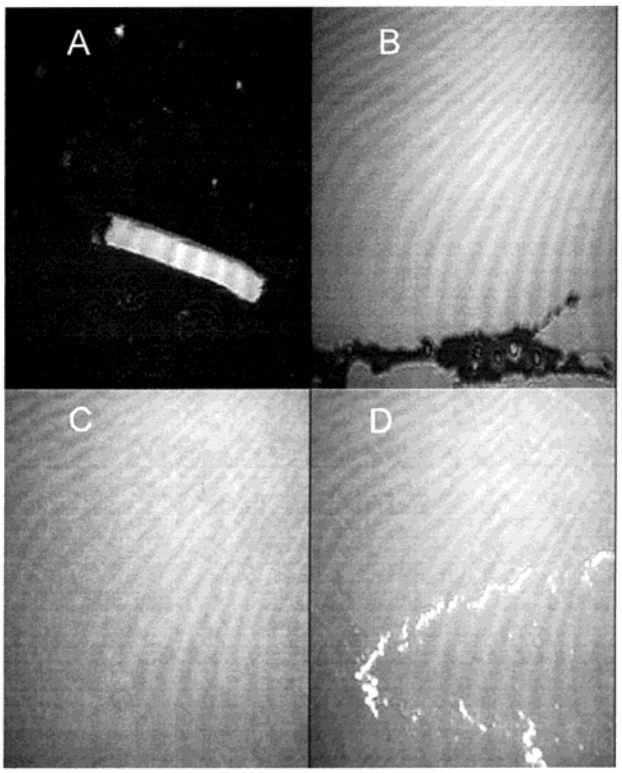

Figure 6. Brewster angle microscopy of a monolayer of BAME at (A) 0 mN/m, (B) 20 mN/m, (C) 30 mN/m, and (D) 40 mN/m. Each image is 625 × 500 μm.

the film. The PM-IRRAS spectra recorded at surface pressure higher than 10 mN/m show the wagging and twisting bands between 1200 and 1350 cm^{-1}. To our knowledge, it is the first observation of the wagging band progression in the infrared spectrum of a Langmuir monolayer. These bands and the band at 1435 cm^{-1} corresponding to the bending vibration of the methyl of the polar head are negative with respect to the baseline, indicating that their transition moments are mostly perpendicular to the plane of the film. The downward orientation of bands due to the wagging and twisting vibrations combined with the upward orientation of the bands due to the stretching and bending vibrations of the methylene groups are consistent with a preferentially perpendicular orientation of the BAME alkyl chains at the air/water interface. The presence of domains at the air/water interface has been confirmed by Brewster angle microscopy measurements on BAME monolayers, as seen in Figure 6. At very low surface pressure ($\pi \approx 0$ mN/m), the monolayer shows large domains with sharp and clearly defined edges (Figure 6A). These domains are observed right after spreading the BAME solution, which indicates that the molecules do not form a gas analogous phase, but directly a solidlike phase. Upon compression, the domains coalesce (Figure 6B) and form a homogeneous monolayer at $\pi = 30$ mN/m (Figure 6C). At higher surface pressures, small bright areas characteristic of multilayer domains are observed.

Discussion

Oscillator Strength of the Methylene C−H Stretching Modes. The anisotropic values of the extinction coefficient ($k_{x,y}$ and k_z) shown in Figure 3B allow calculating the maximum extinction coefficient, k_{max}, which is given, for each wavenumber, by

$$k_{max} = k_x + k_y + k_z \quad (1)$$

TABLE 1: Anisotropic Extinction Coefficients and k_{max} Values for Behenic Acid Methyl Ester (BAME), Cadmium Arachidate (CdAr), and Dimyristoylphosphatidic Acid (DMPA)

	CH_2/chain	band, cm^{-1}	$k_{x,y}$	k_z	k_{max}	k_{max}/CH_2
BAME	20	2918	0.553	0.128	1.234	0.062
			±0.030	±0.004	±0.064	±0.003
		2850	0.372	0.128	0.872	0.044
			±0.020	±0.004	±0.044	±0.002
CdAr[a]	18	2919	0.473	0.023	0.969	0.054
			±0.012	±0.001	±0.025	±0.001
		2850	0.330	0.014	0.674	0.037
			±0.006	±0.001	±0.013	±0.001
DMPA[b]	13	2918	0.278	0.096	0.652	0.050
		2850	0.189	0.065	0.443	0.034

[a] From ref 49. [b] From ref 42.

The value of k_{max} for each band depends on the strength and number of oscillators and on the molecular density of the film. Table 1 lists the values of $k_{x,y}$, k_z and k_{max} for the $\nu_a(CH_2)$ and $\nu_s(CH_2)$ bands of BAME, cadmium arachidate (CdAr)[49] and dimyristoylphosphatidic acid (DMPA).[42] The value of k_{max} per methylene group for the $\nu_a(CH_2)$ band is 0.050 for DMPA, 0.054 for the CdAr and 0.062 for BAME. Similarly, the value of k_{max} per methylene group for the $\nu_s(CH_2)$ band is 0.034, 0.037 and 0.044 for DMPA, CdAr and BAME, respectively. These results show that the values of k_{max} for BAME are about 15% higher than those for DMPA and CdAr. This difference most likely arises from a difference of the density of the surface packing of the methylene groups and is consistent with the quasi-crystalline packing of the BAME films. Flach et al. have estimated a k_{max} value of 1.07 for the $\nu_a(CH_2)$ band of a monolayer of BAME at the air/water interface compressed at 14 mN/m.[28] The discrepancy between their value and the value of 1.23 obtained here most likely arises from a difference in molecular density. These results show that the value of k_{max} significantly depends on the compression of the monolayer and that the molecular density of the film should be considered when data are compared from a study to another.

Orientation of the Alkyl Chain from the Anisotropic Extinction Coefficients. The $k_{x,y}$ and k_z values given in Table 1 also allow to compare qualitatively the orientation of the alkyl chains in the three compounds. For the $\nu_a(CH_2)$ and $\nu_s(CH_2)$ bands of both DMPA and BAME, the value of k_z is about a third of the value of $k_{x,y}$ while for CdAr, the value of k_z is only 5% of the value of $k_{x,y}$. Since the transition moments of the $\nu_a(CH_2)$ and $\nu_s(CH_2)$ bands make an angle of 90° with the molecular axis for the all-trans chain, this suggests that the alkyl chain of CdAr is less tilted from the normal of the film than those of BAME and DMPA.

It is possible to obtain quantitative information about the orientation of alkyl chains assuming a conformation and orientation molecular model. Indeed, for alkyl chains in all-trans conformation and considering both a uniaxial orientation of the molecules and a cylindrical symmetry around the molecular axis, Fraser and McRae derived the following equations that connect the anisotropic extinction coefficients k_x, k_y and k_z with k_{max} and the tilt angle γ of the alkyl chains with respect to the normal surface:[51]

$$k_x = k_y = \left[\frac{f \sin^2 \alpha}{2} + \frac{(1-f)}{3}\right] k_{max} \quad (2)$$

$$k_z = \left[f \cos^2 \alpha + \frac{(1-f)}{3}\right] k_{max} \quad (3)$$

where $f = (3\langle \cos^2 \gamma \rangle - 1)/2$ is the second moment of the

TABLE 2: Anisotropic Extinction Coefficients, Tilt Angles of the Transition Moments (θ), and Molecular Tilt Angle (γ) Calculated from $k_{x,y}$ and k_z for Selected Bands of BAME

band (cm^{-1})	$k_{x,y}$	k_z	k_{max}	θ ($\pm 2°$)	γ ($\pm 2°$)
2918[a]	0.553	0.128	1.234	71	27
2850[a]	0.372	0.128	0.872	68	32
1739[a]	0.252	0.177	0.681	59	
1238[b]	0.0055	0.094	0.105	19	19
1221[b]	0.0058	0.115	0.127	18	18
1205[b]	0.0106	0.185	0.206	19	19
1174[a]	0.0156	0.357	0.388	17	

[a] $k_{x,y}$ and k_z are determined at the peak maximum. [b] $k_{x,y}$ and k_z are the peak heights measured using a baseline drawn from the minima on either side of each peak.

orientation function of the molecular axis, γ is the molecular tilt angle and α is the angle between the transition moment of the considered infrared mode and the alkyl chain axis. For vibrations with a transition moment perpendicular to the chain axis ($\alpha = 90°$), eqs 2 and 3 can be rearranged to calculate γ:

$$\gamma_{\alpha=90°} = \arccos \sqrt{\frac{2k_x - k_z}{2k_x + k_z}} \quad (4)$$

For bands with a transition moment parallel to the chain axis ($\alpha = 0°$) the tilt angle γ is given by

$$\gamma_{\alpha=0°} = \arctan \sqrt{\frac{2k_x}{k_z}} \quad (5)$$

It is noteworthy that eq 5 does not require the cylindrical symmetry around the molecular axis since the transition moment is along the chain axis. In addition, this equation can be used to calculate the tilt angle θ of the transition moment of any vibration. Table 2 shows the molecular tilt angle γ calculated from the $k_{x,y}$ and k_z values using eqs 4 and 5. The molecular tilt angles calculated from the $\nu_a(CH_2)$ and $\nu_s(CH_2)$ bands (i.e., from transition moment perpendicular to the chain axis) are slightly different and both of them are higher than those calculated from bands due to vibration having their transition moment parallel to the chain axis, such as the methylene wagging and twisting vibrations in the 1200−1350 cm^{-1} region. Two reasons can be at the origin of these discrepancies. (i) The first one is the noncylindrical symmetry of the alkyl chains around the molecular axis. Indeed, as observed in Figure 3B, the relative intensity of the $\nu_a(CH_2)$ and $\nu_s(CH_2)$ bands is not the same for $k_{x,y}$ and k_z. Since, the transition moments of both vibrations are perpendicular to the chain axis, the relative value of their projection in the *x, y* and *z* directions should be the same if the alkyl chains have a cylindrical symmetry around the chain axis. Figure 3B shows that it is not the case for BAME. This effect most likely account for the discrepancy between the γ values calculated from the $\nu_a(CH_2)$ and $\nu_s(CH_2)$ bands. (ii) The second reason is the low precision on the determination of the anisotropic extinction coefficients for the wagging and twisting vibrations. The lack of precision is due to the very low intensity of the bands due to these vibrations in the transmittance spectrum used to determine the in-plane extinction coefficients and also to the difficulty in defining of a proper baseline in this spectral region for both p- and s-polarized spectra since the wagging bands overlap strongly. Since the error made on the determination of the molecular tilt angles using eq 5 for the wagging bands is quite high the values obtained are not very accurate, despite the fact that the wagging vibration are not sensitive to the cylindricity of the alkyl chain. Therefore, only the molecular tilt angles calculated from the anisotropic extinction coefficients of the $\nu_a(CH_2)$ and $\nu_s(CH_2)$ bands should be considered. The results obtained indicate that the tilt angle of the alkyl chain of BAME varies from 27 to 32° depending on the infrared mode considered.

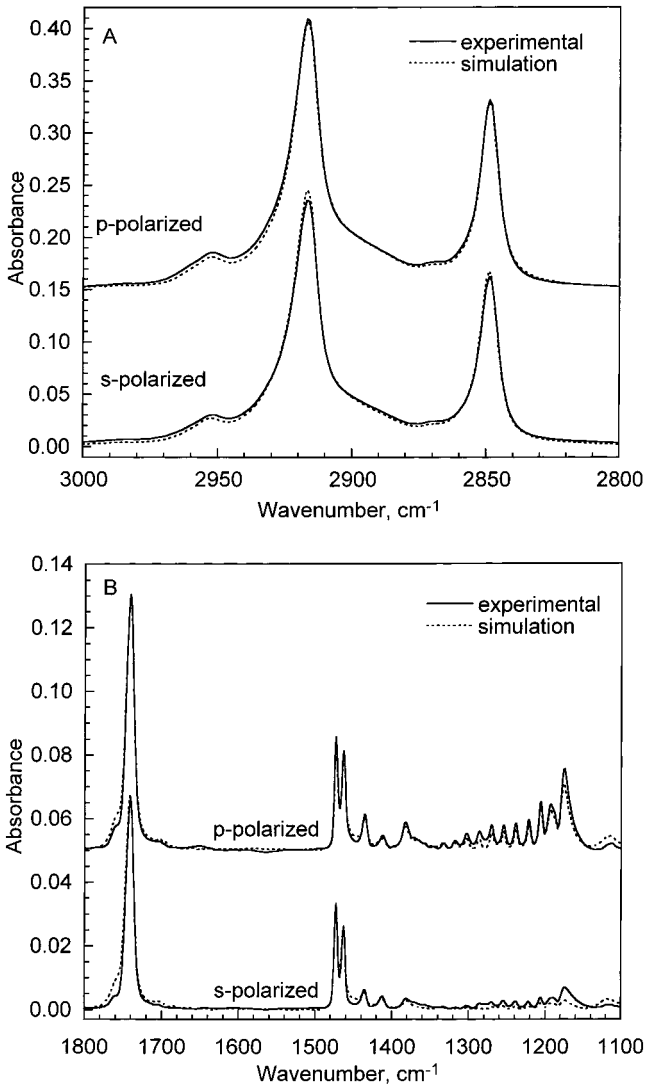

Figure 7. Experimental and simulated ATR spectra of BAME on germanium crystal for (A) the 3000−2800 cm^{-1} region and (B) the 1800−1100 cm^{-1} region.

Orientation of the Alkyl Chain from Polarized ATR. Dichroic ratios obtained from polarized ATR spectra constitute one of the quickest and easiest ways to calculate the molecular orientation of uniaxially oriented thin films.[52,53] To validate the values of the anisotropic optical constants and to verify the molecular orientation of BAME on solid substrates, polarized ATR spectra of a spin-coated BAME film on germanium were recorded. ATR spectra of the film were then simulated using an incidence angle of 45° and considering the first phase as the germanium crystal (real refractive index $n = 4$), the second phase as the BAME film with a thickness of 230 Å and the last phase as air. Polarized ATR spectra were calculated for 12 reflections because the film was deposited only on one side of the crystal. As seen in Figure 7A,B, the agreement between the experimental and simulated spectra is quite good for the for the p-polarized spectrum but show some divergences for the s-polarized spectrum, showing that the orientation of the BAME molecules on the germanium ATR crystal is not exactly the same as that found on other solid substrates.

TABLE 3: Mean Square Electric Field Amplitudes ($\langle E_y^2\rangle$, $\langle E_x^2\rangle$, and $\langle E_z^2\rangle$), Dichroic Ratio (R_{ATR}) and Tilt Angle of the Transition Moments (θ_{ATR}) and Molecular Tilt Angle (γ_{ATR}) Calculated for Selected Bands of BAME

band (cm^{-1})	$\langle E_x^2\rangle$	$\langle E_y^2\rangle$	$\langle E_z^2\rangle$	R_{ATR}	θ_{ATR} ($\pm 2°$)	γ_{ATR} ($\pm 2°$)
2918	1.889	1.947	0.649	1.099	66	35
2850	1.892	1.951	0.647	1.115	65	37
1739	1.931	2.018	0.619	1.214	57	
1238	1.949	2.050	0.606	3.256	27	27
1221	1.949	2.051	0.606	3.866	24	24
1205	1.950	2.052	0.606	4.083	24	24
1174	1.951	2.054	0.605	3.717	25	

Experimental ATR spectra were also used to calculate the molecular orientation using the dichroic ratios method.[44,52,53] In this method, the order parameter S_z is calculated for the transition dipole moment of the selected mode using the following equation:

$$S_z = \frac{\langle E_x^2\rangle - \langle E_y^2\rangle R_{ATR} + \langle E_z^2\rangle}{\langle E_x^2\rangle - \langle E_y^2\rangle R_{ATR} - 2\langle E_z^2\rangle} \tag{6}$$

where $\langle E_x^2\rangle$, $\langle E_y^2\rangle$ and $\langle E_z^2\rangle$ are the mean square electric field (MSEF) amplitudes of the evanescent polarized radiation in the film and R_{ATR} is the dichroic ratio ($R_{ATR} = A_p/A_s$). The MSEF were calculated exactly using thickness- and absorption-dependent equations.[42,54,55] The tilt angle of the transition dipole moment is given by the relation

$$\theta_{ATR} = \arccos\sqrt{\frac{2S_z + 1}{3}} \tag{7}$$

The orientation of the alkyl chain was also calculated from the order parameter S_z using the Legendre addition theorem:

$$f = \frac{3\langle\cos^2\gamma\rangle - 1}{2} = \frac{2S_z}{3\cos^2\alpha - 1} \tag{8}$$

The values of $\langle E_x^2\rangle$, $\langle E_y^2\rangle$ and $\langle E_z^2\rangle$, of the dichroic ratio, θ_{ATR}, and γ_{ATR} calculated with this method for several bands are given in Table 3. These results show unambiguously that the BAME molecules are also tilted on the ATR crystal as observed from the anisotropic extinction coefficients. However, the values of the molecular tilt angle calculated from the ATR polarized spectra are slightly higher than those determined from the anisotropic extinction coefficients, indicating that the alkyl chains are more tilted when BAME is deposited onto germanium crystal. This result is corroborated by a higher intensity of the wagging and twisting bands in the experimental s-polarized ATR spectrum compared to the simulated one.

Organization of BAME Molecules. Infrared spectra of BAME deposited on solid substrates and at the air/water interface reveal a splitting of the bands due to the methylene bending and rocking vibrations, suggesting that the film adopts a quasi-crystalline structure. In a previous study, Flach et al. made the hypothesis that the structure of BAME at the air/water interface was orthorhombic with no tilt angle of the hydrocarbon chains rather than monoclinic.[28] The difference between these two crystalline structures is the tilt of the chains in the monoclinic structure. The infrared spectra for these two structures should show a splitting of the bands due to the bending and rocking modes of the methylene groups, arising from the intermolecular coupling between the methylene groups. The exact nature of the crystal lattice, orthorhombic or monoclinic, cannot be determined directly from the infrared spectra, because of their nearly identical subcell units. Generally, fatty acids,[56−59] fatty acid methyl or ethyl esters[60,61] and particularly behenic acid methyl ester[62] adopt a monoclinic structure in which the hydrocarbon chains are tilted. The tilt angle is normally near 30° for fatty acids and a value of 26.5° has been found for the stearic acid methyl ester in the solid state by X-ray diffraction.[60] These results are consistent with those obtained from the anisotropic extinction coefficients or from the polarized ATR spectra that indicate that the tilt angle of the BAME molecules is near 30° on solid substrates. Therefore, when ultrathin film of BAME are spin-coated onto solid substrates, an organization of BAME molecules close to that of the crystal structure is obtained. A similar behavior was also observed for spin-coated thin phospholipid films.[63]

PM-IRRAS of BAME at the Air/Water Interface. Since the existence of large domains observed by Brewster angle microscopy and the splitting of the methylene bending mode in PM-IRRAS spectrum suggest that the BAME molecules are packed in a quasi-crystalline structure at the air/water interface, even at low surface pressure, we have verified if the anisotropic optical constants of BAME could be transferred from the solid films to the air/water interface. The PM-IRRAS spectrum of a monolayer at the air/water interface has been simulated and compared with that observed experimentally at a surface pressure of 30 mN/m. The normalized spectrum S(d)/S(0) has been calculated using the anisotropic optical constants of BAME presented in Figure 3 and the isotropic optical constants of water determined by Bertie and Lan.[64] The thickness of the monolayer was taken equal to 30.6 Å.[28] Figure 8 shows that the PM-IRRAS of BAME is not very well reproduced by the spectrum calculated using the anisotropic optical constants. In the low-frequency region, the major differences come from bands associated with the polar headgroup region. For example, the negative band due to the bending of the methyl group of the polar head (1435 cm^{-1}) is weaker and shifted in the simulated spectrum. The band due to the C═O vibration is narrower and is also slightly shifted on the simulated spectrum. The negative band due to the C—O—C stretching vibration (1174 cm^{-1}) is also much weaker in the experimental spectrum. All these observations indicate that the polar head has not the same orientation at the air/water interface and on a solid substrate, presumably as a result of the hydration of the polar head. Differences are also observed for the bands due to the hydrophobic moiety of the BAME molecule. The splitting of the $\delta(CH_2)$ band is well reproduced except for the relative intensity of its two components. The 1411 cm^{-1} band, due to the methyl bending mode, is well reproduced while the bands due to the methylene wagging and twisting modes are weaker and broader in the experimental PM-IRRAS spectrum than the simulated one. These differences between the two spectra may also be due to different environments for the polar heads on solid substrates and at the water surface, which affect the oscillator strengths of the wagging and twisting modes.

Figure 8A shows that in the C—H stretching region, the calculated spectrum is significantly lower in intensity than the experimental one recorded at $\pi = 30$ mN/m. The intensity of the 2918 and 2850 cm^{-1} bands in the simulated PM-IRRAS spectrum is 1.0153 and 1.0107, respectively, compared to values of 1.0179 ± 0.0004 and 1.0141 ± 0.0003 obtained experimentally for the 2918 and 2850 cm^{-1}, respectively, from the average of 18 spectra recorded at $\pi = 30$ mN/m. This result indicates that the optical constants obtained from spin coated films on solid substrates cannot be transferred directly to the air/water interface. The lower intensity obtained in the simulated spectrum

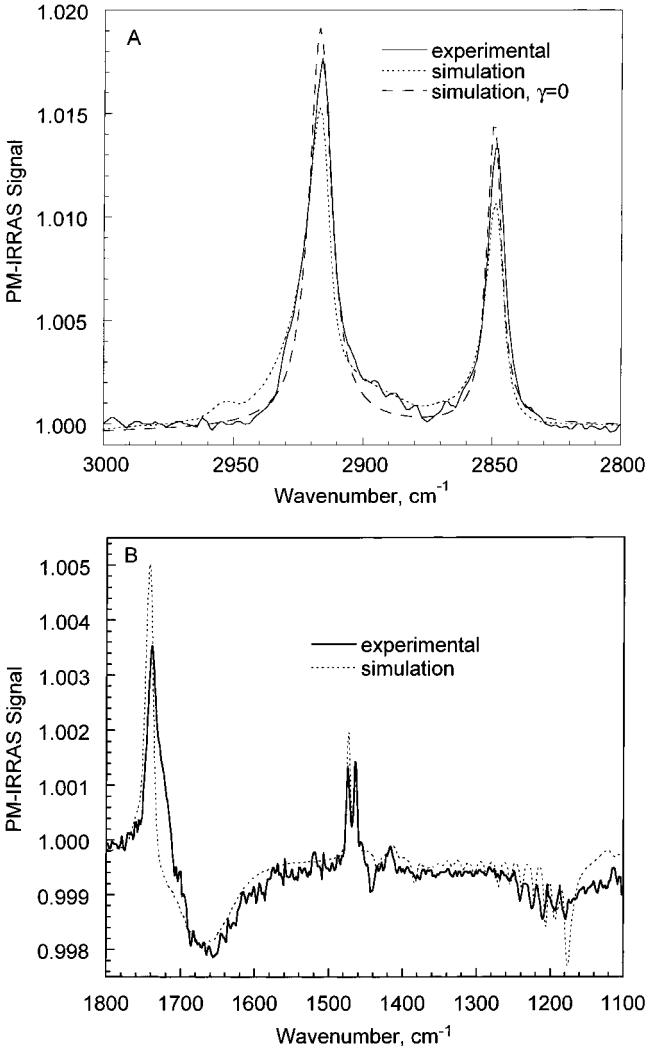

Figure 8. Experimental and simulated PM-IRRAS spectra of BAME at the air/water interface for (A) the 3000−2800 cm^{-1} region and (B) the 1800−1100 cm^{-1} region. To obtain this spectrum, the photoelastic modulator was set to introduce a maximum dephasing at 2000 cm^{-1}. For comparison, a PM-IRRAS spectrum in the C−H region simulated for a tilt angle of 0° is also shown. This spectrum was calculated using the k_{max} values given in Table 1 for two bands located at 2918 and 2850 cm^{-1} with Lorentzian band shape and full width at half-height of 11 and 7 cm^{-1}, respectively.

can be due either to higher extinction coefficients (k_{max}) for the methylene stretching vibrations or to a lower tilt angle of the alkyl chain at the air/water interface. Since the results obtained by infrared spectroscopy and Brewster angle microscopy show that the BAME molecules are packed in a quasi-crystalline structure at the air/water interface with alkyl chains in the all-trans conformation, there is no compelling reason to believe that the values of k_{max} are different on solid substrates and at the air/water interface. To verify the effect of tilt angle, we have simulated a PM-IRRAS spectrum in the C−H region using the k_{max} values given in Table 1 for the bands located at 2918 and 2850 cm^{-1} but for a tilt angle of 0° by transferring the k_{max} values along the film surface ($k_x = k_y = 0.617$ and $k_z = 0$ for the 2918 cm^{-1} band and $k_x = k_y = 0.436$ and $k_z = 0$ for the 2850 cm^{-1} band). As seen in Figure 8A, the simulated spectrum is much closer to that obtained experimentally, the simulated PM-IRRAS normalized intensity for the 2918 and 2850 cm^{-1} bands being 1.0183 and 1.0143, respectively. This simulation strongly suggests that the tilt angle of the alkyl chain of BAME is close to 0° as opposed to a tilt angle of about 30° obtained for the films deposited on solid substrates in agreement with the results obtained by Flach et al.[28] This difference in tilt angle can also explain some of the changes observed in the low-frequency region.

Conclusion

The in-plane and out-of-plane optical constants of a BAME ultrathin film have been determined from a transmittance spectrum at normal incidence and a p-polarized IRRAS spectrum at grazing incidence, respectively. The anisotropic extinction coefficients and the polarized ATR spectra were used to calculate the tilt angle of several transition moments and also the molecular tilt angle of BAME assuming an all-trans conformation of the alkyl chain. The results indicate that the alkyl chain of the fatty acid ester is tilted and that the molecular tilt angle is close to 30°, as observed for other fatty acid methyl esters in the crystalline state. The splitting of the methylene bending mode and the presence the band progression due to the methylene wagging modes in the PM-IRRAS spectra of Langmuir monolayers of BAME show that the all-tans alkyl chains are packed in a quasi-crystalline structure at the air/water interface, even at low surface pressure. These findings were further confirmed by Brewster angle microscopy. Nevertheless, the simulation of the PM-IRRAS spectrum of a BAME monolayer recorded at 30 mN/m indicates that the optical constants obtained from films prepared by spin-coating cannot be transferred directly to the air/water interface. The simulation reveals that, as opposed to the tilted orientation found on solid substrates, the alkyl chain of BAME is nearly perpendicular to the air/water interface in Langmuir films.

Acknowledgment. We thank France Fréchette for her technical assistance for the synthesis of the deuterated BAME sample. This work was supported in part by the Natural Sciences and Engineering Research Council of Canada (NSERC), by the Fonds pour la Formation de Chercheurs et pour l'aide à la Recherche (Fonds FCAR) of the Province of Québec and by the Centre National de la Recherche Scientifique (CNRS, Département Sciences Chimiques). I.P. is also grateful to NSERC and Fonds FCAR for postgraduate scholarships.

References and Notes

(1) Tredgold, R. H.; Young, M. C. J.; Hodge, P.; Khoshdel, E. *Thin Solid Films* **1987**, *151*, 441.
(2) Honeybourne, C. T. *Chem. Solids* **1987**, *48*, 109.
(3) Moriizumi, T. *Thin Solid Films* **1987**, *152*, 345.
(4) Seto, J.; Nagai, T.; Ishimoto, C.; Watanage, N. *Thin Solid Films* **1985**, *134*, 101.
(5) Lavigne, P.; Tancrède, P.; Lamarche, F.; Grandbois, M.; Salesse, C. *Thin Solid Films* **1994**, *242*, 229.
(6) Gutberlet, T.; Vollhardt, D. *J. Colloid Interface Sci.* **1995**, *173*, 429.
(7) Cuvillier, N.; Mingotaud, C.; Ikegami, K. *J. Chem. Phys.* **1999**, *111*, 6982.
(8) Fukuto, M.; Hellermann, R. K.; Pershan, P. S.; Yu, S. M.; Griffiths, J. A.; Tirrell, D. A. *J. Chem. Phys.* **1999**, *111*, 9761.
(9) Flach, C. R.; Mendelsohn, R.; Rerek, M. E.; Moore, D. J. *J. Phys. Chem. B* **2000**, *104*, 2159.
(10) Sigiyama, N.; Shimizu, A.; Nakamura, M.; Nakagawa, Y.; Nagasawa, Y.; Ishida, H. *Thin Solid Films* **1998**, *331*, 170.
(11) Deleu, M.; Paquot, M.; Jacques, P.; Thonart, P.; Adriaensen, Y.; Dufreme, Y. F. *Biophys. J.* **1999**, *77*, 2304.
(12) Morita, S.-I.; Iriyama, K.; Ozaki, Y. *J. Phys. Chem. B* **2000**, *104*, 1183.
(13) Watts, A.; Harlos, K.; Marsh, D. *Biochim. Biophys. Acta* **1981**, *645*, 91.
(14) Nicklow, R. M.; Romerantz, M.; Segmüller, A. *Phys. Rev.* **1981**, *23*, 1081.
(15) Hithfiels, R. R.; Thomas, R. K.; Cummins, R. G.; Gregory, D. P.; Mingins, J.; Hayter, J. B.; Schärpf, O. *Thin Solid Films* **1983**, *99*, 165.

(16) Subirade, M.; Lebugle, A. *Thin Solid Films* **1994**, *243*, 442.
(17) Takamura, T.; Matsushita, K.; Shimoyama, Y. *Jpn. J. Appl. Phys.* **1996**, *35*, 5831.
(18) Millela, E.; Giannini, C.; Tapfer, L. *Thin Solid Films* **1997**, *293*, 291.
(19) Gallant, J.; Desbat, B.; Vaknin, D.; Salesse, C. *Biophys. J.* **1998**, *75*, 2888.
(20) Dluhy, R. A. *J. Phys. Chem.* **1986**, *90*, 1373.
(21) Dluhy, R. A.; Wright, N. A.; Griffiths, P. R. *Appl. Spectrosc.* **1988**, *42*, 138.
(22) Gericke, A.; Huhnerfuss, H. *J. Phys. Chem.* **1993**, *97*, 12899.
(23) Gericke, A.; Michailov, A. V.; Huhnerfuss, H. *Vibr. Spectrosc.* **1993**, *4*, 335.
(24) Gericke, A.; Huhnerfuss, H. *Thin Solid Films* **1994**, *245*, 74.
(25) Mendelsohn, R.; Brauner, J. W.; Gericke, A. *Annu. Rev. Phys. Chem.* **1995**, *46*, 305.
(26) Pastrana Rios, B.; Taneva, S.; Keough, K. M.; Mautone, A. J.; Mendelsohn, R. *Biophys. J.* **1995**, *69*, 2531.
(27) Gericke, A.; Brauner, J. W.; Erukulla, R. K.; Bittman, R.; Mendelsohn, R. *Thin Solid Films* **1997**, *292*, 330.
(28) Flach, C. R.; Gericke, A.; Mendelsohn, R. *J. Phys. Chem. B* **1997**, *101*, 58.
(29) Blaudez, D.; Buffeteau, T.; Cornut, J. C.; Desbat, B.; Escafre, N.; Pézolet, M.; Turlet, J. M. *Appl. Spectrosc.* **1993**, *47*, 869.
(30) Blaudez, D.; Buffeteau, T.; Cornut, J. C.; Desbat, B.; Escafre, N.; Pézolet, M.; Turlet, J. M. *Thin Solid Films* **1994**, *242*, 146.
(31) Sato, Y.; Frey, B. L.; Corn, R. M.; Uosaki, K. *Bull. Chem. Soc. Jpn.* **1994**, *67*, 21.
(32) Blaudez, D.; Turlet, J.-M.; Dufourcq, J.; Bard, D.; Buffeteau, T.; Desbat, B. *J. Chem. Soc., Faraday Trans.* **1996**, *92*, 525.
(33) Cornut, I.; Desbat, B.; Turlet, J.-M.; Dufourcq, J. *Biophys. J.* **1996**, *70*, 305.
(34) Mao, L.; Ritcey, A. M.; Desbat, B. *Langmuir* **1996**, *12*, 4754.
(35) Huo, Q.; Dziri, L.; Desbat, B.; Russell, K. C.; Leblanc, R. M. *J. Phys. Chem. B* **1999**, *103*, 2929.
(36) Buffeteau, T.; Le, C. E.; Castano, S.; Desbat, B.; Blaudez, D.; Dufourcq, J. *J. Phys. Chem. B* **2000**, *104*, 4537
(37) Takenaka, T.; Harada, K.; Matsumoto, M. *J. Colloid Interface Sci.* **1980**, *73*, 569.
(38) Takeda, F.; Matsumoto, M.; Takenaka, T.; Fujiyoshi, Y. *J. Colloid Interface Sci.* **1981**, *84*, 220.
(39) Ahn, D. J.; Franses, E. I. *J. Phys. Chem.* **1992**, *96*, 9952.
(40) Ahn, D. J.; Franses, E. I. *Thin Solid Films* **1994**, *244*, 971.
(41) Bechinger, B.; Ruysschaert, J.-M.; Goormaghtigh, E. *Biophys. J.* **1999**, *76*, 552.
(42) Picard, F.; Buffeteau, T.; Desbat, B.; Auger, M.; Pezolet, M. *Biophys. J.* **1999**, *76*, 539.
(43) Goormaghtigh, E.; Raussens, V.; Ruysschaert, J.-M. *Biochim. Biophys. Acta* **1999**, *1422*, 105.
(44) Buffeteau, T.; Le Calvez, E.; Desbat, B.; Pelletier, I.; Pezolet, M. *J. Phys. Chem. B* **2001**, *105*, 1464.
(45) Takenaka, T.; Umemura, J.; Kamata, T.; Kawai, T.; Koizumi, N. *Polym. J.* **1991**, *23*, 357.
(46) Hasegawa, T.; Takeda, S.; Kawaguchi, A.; Umemura, J. *Langmuir* **1995**, *11*, 1236.
(47) Hagting, J. G.; Vorenkamp, E. J.; Schouten, A. J. *Macromolecules* **1999**, *32*, 6619.
(48) Chernyshova, I. V.; Rao, K. H. *J. Phys. Chem. B* **2001**, *105*, 810
(49) Buffeteau, T.; Blaudez, D.; Péré, E.; Desbat, B. *J. Phys. Chem. B* **1999**, *103*, 5020.
(50) Snyder, R. G. *J. Mol. Spectrosc.* **1961**, *7*, 116.
(51) Fraser, R. D. B.; MacRae, T. P. *Conformation in Fibrous Proteins and Related Synthetic Polypeptides*; Academic Press: New York, 1973.
(52) Fringeli, U. P.; Günthard, H. H. Infrared membrane spectroscopy. In *Membrane Spectroscopy*; E. Grell, Ed.; Springer-Verlag: New York, 1981.
(53) Axelsen, P. H.; Kaufman, B. K.; McElhaney, R. N.; Lewis, R. N. A. H. *Biophys. J.* **1995**, *69*, 2770.
(54) Hansen, W. H. J. *J. Opt. Soc. Am.* **1968**, *58*, 380.
(55) Axelsen, P. H.; Citra, M. *Prog. Biophys. Mol. Biol.* **1997**, *66*, 227.
(56) Sydow, E. V. *Acta Crystallogr.* **1955**, *8*, 557.
(57) Sydow, E. v. *Acta Crystallogr.* **1955**, *8*, 810.
(58) Sydow, E. v. *Acta Chem. Scan.* **1955**, *10*, 1685.
(59) Sydow, E. v. *Ark. Kemi* **1956**, *19*, 231.
(60) Aleby, S.; Sydow, E. v. *Acta Crystallogr.* **1960**, *13*, 487.
(61) Aleby, S. *Acta Crystallogr.* **1962**, *15*, 1248.
(62) Aleby, S. *Ark. Kemi* **1969**, *31*, 267.
(63) Le Calvez, E. Développement et applications de la spectroscopie infrarouge à l'étude de systèmes biochimiques modèles. Thèse de doctorat (#2292), Université de Bordeaux I, 2000.
(64) Bertie, J. E.; Lan, Z. *Appl. Spectrosc.* **1966**, *50*, 1047.